Ficha gerada por meio do SIGAA/Biblioteca com dados fornecidos pelo(a) autor(a).
Núcleo Integrado de Bibliotecas/UFMA

Sousa Silva, Arthur Vinicius.
Potencial application of fish scales as feedstock in termochemical processes for the clean energy generation / Arthur Vinicius Sousa Silva. - 2019.
31 p.

Orientador(a): Glauber Cruz.
Curso de Engenharia Mecânica, Universidade Federal do Maranhão, Centro Pedagógico Paulo Freire, sala 308 Asa norte, 2019.

1. Bioenergy. 2. Biomass. 3. Collagen. 4. Fishery residues. I. Cruz, Glauber. II. Título.

Universidade Federal do Maranhão
Centro de Ciências Exatas e Tecnológicas
Curso Bacharelado em Engenharia Mecânica

Potential application of fish scales as feedstock in thermochemical processes for the clean energy generation

São Luís / MA
2019

Universidade Federal do Maranhão
Centro de Ciências Exatas e Tecnológicas
Curso Bacharelado em Engenharia Mecânica

Potential application of fish scales as feedstock in thermochemical processes for the clean energy generation

Artigo apresentado ao Curso Bacharelado em Engenharia Mecânica como pré-requisito para a obtenção do título de Bacharel em Engenharia Mecânica.

Discente: Arthur Vinicius Sousa Silva
Orientador: Prof. Dr. Glauber Cruz

São Luís / MA
2019

Abstract

The replacement of fossil fuels by renewable sources has been discussed globally, since these accounts for a large pollutant emissions part into the atmosphere. Several cities of the Brazilian coast produce a variety of fish types, generating large waste amounts, including viscera and/or fish scales, which are already used in several industrial processes. But these cities still face a large environmental problem, *i.e.*, residues disposal from commercial establishments, for example, fishmongers, which are often discarded in a disordered and/or unplanned manner in inappropriate places. Within this scenario, this research investigated the energy utilization of a collagenous biomass supplied by a fishery in the São Luís city (MA), when it is submitted to combustion (synthetic air) and pyrolysis (100% N_2) processes for the bioenergy generation. Physicochemical properties from fish scales were evaluated by proximate and ultimate analyzes, scanning electron microscopy (SEM), energy dispersive spectroscopy (EDS), X-Ray diffraction (XRD), Fourier transform infrared spectroscopy (FTIR) and inductively couple plasma - optical emission spectroscopy (ICP-OES). The thermal behavior of samples was evaluated by thermogravimetry/ thermogravimetry derivative (TG/DTG), differential thermal analysis (DTA) and calorimetry (HHV/HLV). It was verified that the fish scales has carbon and oxygen contents as major elements, insignificant contents of sulfur and heavy metals (lead, copper, chromium, lithium and zinc). This material also presented a large amorphous region (89%), in addition to collagen fibers presence and hydroxyapatite crystals. It was possible for evaluating the thermal and physicochemical characteristics of this material, compare it to other biomasses already used and predict its use for the bioenergy generation.

Keywords: biomass; fishery residues; bioenergy; collagen.

1) Introduction

Fossil fuels, such as oil, coal and natural gas, represent primary energy sources and account for 80% of world demand (EPE, 2018). At last decades, there has been a growing worldwide consensus that fossil fuels are responsible for promoting environmental damage and, as a consequence, climate change on the Planet and directly interferes in human health, animal and plant (Lela et al., 2015; Williams et al., 2012). Development of new technologies aims to mitigate this situation and a promising alternative is use of renewable fuels for the bioenergy production (Babu, 2008).

The different solid residues generated by several industries and in some domestic cases are classified into three categories: (1) forest residues (wood chips, sawdust, barks, slabs, stems, branches); (2) agricultural residues (bagasse, straw and husks) and (3) urban biomass - originating from municipal, institutional, commercial and industrial solid wastes (treated wood, train tracks and concrete of energy poles) (Saidur et al., 2011; Mckendry, 2002).

Biomasses are known as energy potential sources of a sustainable way, and can be converted directly into heat, electricity or transformed into solid, liquid or gaseous fuels, with great chances of being used as feedstock for the electric energy production, fuel cells and steam generation for gas turbines (Mckendry, 2002). Numerous alternatives have been proposed to increase the biomass amount used for the energy production in the World (Svoboda et al., 2009). These can also be converted into energy useful forms, using thermochemical or biochemical processes (Wanget al., 2006). However, biomass thermochemical conversion technology is dominant due to high efficiency, being the most used combustion, gasification and pyrolysis (Foletto et al., 2005).

Many studies have been carried out to elucidate the various thermochemical conversion processes of biomasses (Poletto et al., 2012; Sanchez-Silva et al., 2012; Saidur et al., 2011; Saddawi et al., 2010; Babu, 2008; Yang et al., 2007; Leroy et al., 2006).Among studies existent in literature on the thermal behavior of small-scale or laboratory biomasses, most important are those performed by Thermal Analysis (TG/DTG and DTA). These techniques allow obtaining information on the of thermal degradation stages of the different materials in simple, fast and direct way. The evaluation of some solid residues by thermoanalytical techniques plays an important role in the understanding of the thermal performance of these materials as biofuels in industrial processes (Chen and Kuo, 2011).

A good combustion system, in addition to a highly simple and efficient operation, must meet to the requirements to minimize environmental impacts. The quantity and pollutants quality emitted in the combustion depend on several factors, for example, fuels analysis, burners design and operation conditions. Even that sulfur (S) and chlorine (Cl) contents in biomasses are lower (Spliethoff, 2010) and, in some cases these are lower than in fossil fuels, the SO_2 (sulfur dioxide) emissions and HCl (hydrochloric acid) in most combustion cases, can not be neglected, even whether some authors state otherwise (Permchart and Koupriano, 2004; Werther et al., 2000).

Currently, several biomasses from agricultural residues (soybean, rice, coffee and sugarcane bagasse) or urban solids (resulting from domestic and commercial activity of the large centers) has been studied by means of thermoconversion processes (Fernández et al., 2012; Garcia et al., 2012; Kanzac et al., 2011). Some of these biomasses already are being tested in thermal or laboratory-scale plants and could be used to replace fossil fuels in a near future (Cruz, 2015).

Whether different biomasses are used as an important source of alternative energy, then a more detailed understanding of the physicochemical properties and thermal conversion processes is necessary, especially regarding to the performance and atmospheric pollutants formation during these processes (Wiliams et al., 2012).

Saidur (2011) and Mckendry (2002) reported that, as well as the various industrial and domestic segments, some extractive activities, such as fishing, also generate a large disposable materials amount, for example, scales and viscera.

Fish production in the Maranhão State is one of the most representative economic activities from the Brazilian coast, not only for quantity (tons), but also for species diversity (Almeida, 2008). Productivity of yellow fished (*Cynoscion acoupa*), the most appreciated by local population, for example, it was estimated at 10,600 tons $year^{-1}$ (Almeida, 2008), while tilapia (*Oreochromis niloticus*), with 2,650 tons $year^{-1}$ at 2018 (ABP, 2018). According to survey conducted by Brazilian Fisheries Association (ABP, 2018), which reported that fish production in the Maranhão State reached 26,500 tons at 2017.

During fishes processing, from 20 to 80% rejects are generated, depending on the processing level and fish types (Bhagwat and Dandge, 2016; Pickler and Filho, 2017; Sockalingam and Abdullah, 2015). The fish scales correspond from 2 to 4% of the dry residues (Ghaly et al., 2013). In its largely, these organic matter remains are discarded

in disordered or unplanned manner in inappropriate places. In fishery activity, fish scales are usually discarded in dumps or dumped at the sea (Ghaly et al., 2013).

The material discarded represents around 50% initial feedstock, which will not be used at the fish final processing (Leite et al., 2016). Approximately 120 million tons $year^{-1}$ of fish residues (fins, bones, scales, viscera etc) are disposed unduly into environment (Jun et al., 2004).

These materials are great importance for various industrial sectors, including textiles, detergents, cosmetics, as well as for scientific and analytical research (Daboor et al., 2012). Fish scales are biocomposites composed to two phases: an organic, containing high proteins such as collagen (Huang et al., 2016), keratin and mucin, whose contents are different for each fish species (Sockalingam and Abdullah, 2015). Second phase, inorganic nature, is composed of hydroxyapatite and calcium carbonate contents (Martins et al., 2015, Sockalingam and Abdullah, 2015).

As in previously cited examples, present paper proposes a sustainable and environmentally friendly reuse of the fish scales (generally) biomass as a possible alternative energy source under thermochemical conversion processes (combustion and pyrolysis), for the bioenergy generation by means of the characterization of its physicochemical properties and thermal behavior.

2) Materials and Methods

2.1 Samples Preparation

The fish scales were provided by a fishmonger from São Luís city (Maranhão State, Northeast region, Brazil), located at 2°31'51" South (latitude) and 44°18'24" West (longitude) (DB CITY, 2019). Scales of various species were used for generalized analysis. The samples were then washed in running water to remove impurities, dried in an oven (average temperature of 70 °C for 48 hours) to remove the excess of moisture, and subjected to grinding and sieving for the selection of granulometry (Cruz, 2015). Thus, two samples with average granulometries of 0.363 mm and 0.300 mm were prepared (Figure 1 a-b).

Fig. 1. Fish scales samples: (a) *in natura* and (b) average granulometry (≈ 0.363 mm).

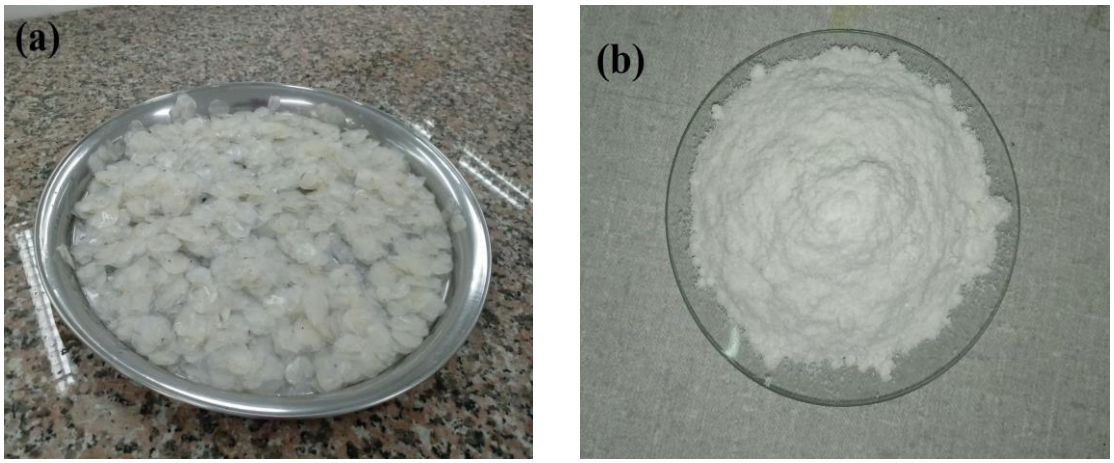

2.2 Proximate analysis

The content of moisture, volatile materials (condensable and non-condensable), fixed carbon and ash of the biomass samples were obtained by means of thermogravimetric analysis in a SDT 2960 Simultaneous TGA-DTA equipment, based on the new methodology developed by Torquato et al. (2017).

2.3 Ultimate analysis

The relative content of carbon (C), hydrogen (H), nitrogen (N) and sulfur (S) present in biomasses were quantified in a 2400 CHNS-O Elemental Analyzer (Perkin Elmer brand), using 2.0 ± 0.5 mg of sample. The oxygen content was quantified by difference at 100%, taking into consideration the other components provided by this analysis, as proposed by Ghetti et al. (1996). The other method here considered was proposed by Roy and Corscadden (2012), besides the ultimate analysis, also consider the content of moisture and ashes, obtained by proximate analysis.

2.4 Calorimetry Analysis

The higher heating value (HHV) of the samples was determined in an IKA C200 calorimeter pump established by ASTM E711 (ASTM, 1987) and NBR 8633 (ABNT, 1984). Equation 1 was used to calculate the LHV (Lower Heating Value) based on the

experimental HHV, ultimate (hydrogen content) and proximate analysis (moisture content) and thermodynamic balance (Cortez et al., 2008).

$$LHV = [(HHV - \lambda * (r + 0.09 * H)) * (100 - W) /100] \quad (1)$$

where λ is the latent heat of water vaporization (2.31 MJ kg^{-1}) at 25 °C, *W* is moisture contained in sample, *H* is the hydrogen content obtained from ultimate analysis and r = W/(100-W), which is denominated of moisture ratio. The calorimetric analysis experiments were performed duplicate and average values are presented.

2.5 Thermal Analysis (TG/DTG and DTA)

The thermal degradation stages of the main constituents of the fishery residues were analyzed by thermogravimetric analysis/derivative thermogravimetric analysis (TGA/DTA) and differential thermal analysis (DTA) under oxidizing (combustion - N_2/O_2: 80/20%) and inert (100% N_2) atmospheres, using a SDT 2960 Simultaneous TGA-DTA thermal analyzer. A dynamic atmospheric flow of 100 mL min^{-1} was applied for both atmospheres, using a sample mass of 7.07 ± 0.01 mg and a heating rate of 10 °C min^{-1} from room temperature to 1000 °C.

2.6 Energy Dispersive Spectroscopy (EDS)

For this specific analysis, samples were placed into a hydraulic press and were secured to an aluminum support by a double side adhesive tape fabricate of carbonaceous material for better fixation during referred analysis. A scanning electronic microscope (Leo Electron Microscopy, LEO440 model) was used to perform the energy dispersive spectroscopy analysis, without previous coating (gold or graphite). This analysis was performed in triplicate for a better results reproducibility.

2.7 Determination of metal composition (ICP-OES)

The concentration of the main inorganic and metallic elements present in fish scales was determined by an inductively coupled plasma - optical emission spectrometer (ICP-OES 710ES model and Varian brand).

2.8 Fourier Transform Infrared Spectroscopy (FTIR)

The FTIR spectra were recorded between 4000 and 400 cm^{-1} in a Shimadzu Fourier transform spectrophotometer (IR-Prestige-21 model), programmed in transmittance mode. The analyses were carried out in KBr pellets for the granulometries of 0.363 mm and lower than 0.300 mm.

2.9 X-Ray Diffraction (XRD)

The crystallographic structures of the samples were evaluated by X-ray diffraction (XRD), using a Bruker brand diffractometer (D8 Advance model), employing CuKα radiation (λ = 1.541 Å, 40 kV - 40 mA). The 2θ ranged from 5° to 70°, with a step size of 0.05° s^{-1}.

The values of the interplanar spacings were calculated from the diffraction angles using Bragg Law, determinate by Equation 2 (Callister, 2002):

$$d = \frac{nk}{2sen(\theta)} \quad (2)$$

Where *n* represents the reflection order, being an integer. It was adopted *n* = 1 and wavelength *k* = 0.154 nm, referring to the CuKα radiation.

The crystallinity index (CI) was calculated by Equation 3 (Yu et al., 2009), where I_{002} is the crystalline region intensity and I_{am} is the amorphous region intensity present in samples. The analyses were performed for particle sizes of 0.363 mm and lower than 0.300 mm.

$$CI = \frac{I_{002} - I_{am}}{I_{002}} x100 \quad (3)$$

2.10 Scanning Electron Microscopy (SEM images)

SEM images were obtained on a LEO440 scanning electronic microscope (Leo Electron Microscope). The biomasses were deposited on an aluminum support previously prepared with a double side adhesive tape produced from carbonaceous

material and submitted to a gold bath. The images were obtained at 200, 500 and 1000 times of magnification.

3) Results and Discussion

3.1 Proximate analysis

Figure 2 shows the proximate analysis profiles obtained for the fish scale samples. According to Yao et al. (2005), for the biomasses in general, proximate analysis is expected to present moisture contents close to 10%, volatile materials from 65 to 85%, ash contents from 5 to 20% and fixed carbon from 7 to 20%.

Fig. 2. Experimental procedure from the proximate analysis obtained by Thermal Analysis for the fish scales.

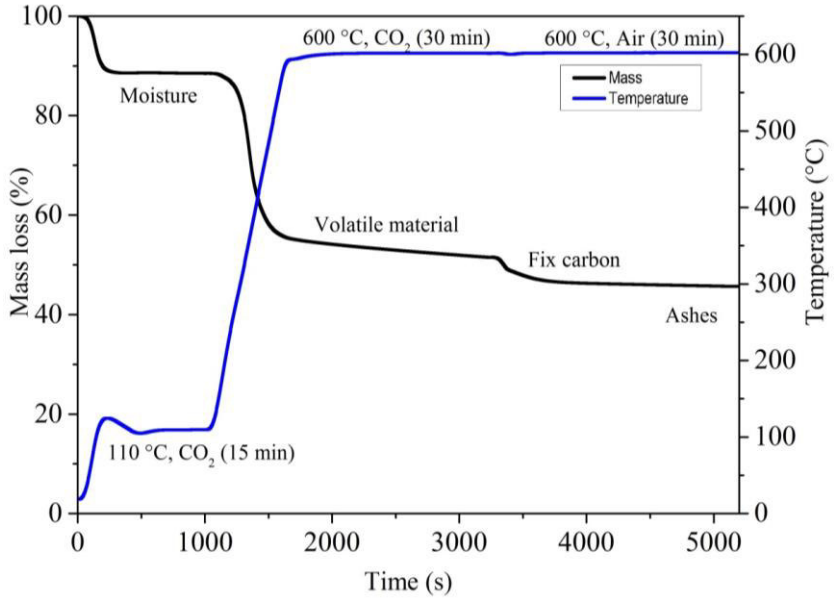

Table 1 shows the properties of proximate analysis obtained for different kinds of biomass. The moisture content around 11%, was close to that found in literature for other kind of biomass, for example, pea husk. This value is considered as appropriate for the application of biomasses under combustion, since biofuels with high moisture contents present lower heating value and, therefore, low energetic performance on boilers (Garcia et al., 2012). Biomass samples with around 35% of volatile materials are below the recommended level, but can reach up to 90%, depending on the sample nature (Khan et al., 2009). As the volatile matter content increases, so does the scattering and

diffusion of the combustible gases inside the combustion chamber during thermochemical process, enriching it (Cruz and Crnkovic, 2019; Garcia et al., 2012).

Table 1: Proximate analysis of fish scales in comparison with different biomasses.

Biomasses	Moisture (%)	VM (%)	FC (%)	VM + FC (%)	Ash (%)
Fish scales	11.34±0.00	35.16±0.00	7.59±0.00	42.75±0.00	45.91±0.00
Sugarcane bagasse	6.70±0.00	n.a.	n.a.	88.70±0.00	4.60±0.00
Scrubland pruning	9.70±0.00	74.50±0.00	n.a.	n.a.	30.30±0.00
Pea husk	11.80±0.00	83.00±0.00	12.50±0.00	95.50±0.00	4.50±0.00

n.a. = not available

Source: adapted from Cruz (2015) and Garcia et al. (2012)

The ash content of approximately 46% is higher than the values found for other biomasses available in literature (Table 1) and is outside the range of expected values. According to Raveendran et al. (1995), this composition can be justified by the presence of high silicon content or other inorganic components, mainly alkali metals and alkaline earths, and may present values above 25%. The fixed carbon around 7% is in the range cited by some authors (Cruz, 2015; Garcia et al., 2012) and is a combustible material (biochar) that remains after moisture removal and volatile materials (Cruz, 2015). It is interesting to note that no available data were found in the literature, regarding the proximate analysis of fish scale samples, which could be used for comparative purposes.

3.2 Ultimate analysis

Table 2 shows the percentage values of carbon, hydrogen, nitrogen, sulfur and oxygen provided by ultimate analysis for the fish scale samples. These are the majority components that compose the various solid fuels or biofuels (Garcia et al., 2012).

The C, H and N levels obtained by ultimate analysis are close to those stipulated by Santos (2008), which used fish scales of piau (*Leporinus obtusidens*) a specie abundant in all Brazilian hydrographic basins (Melo and Ropke, 2004), whose values

were 20.16% for carbon; 3.37% for hydrogen and 6.81% for nitrogen. According to Telmo et al. (2010), for the ultimate analysis of a lignocellulosic biomass it is expected that carbon presents values between 47.0 and 54.0%; hydrogen from 5.6 to 7.0%; oxygen from 40.0 to 44.0%; nitrogen from 0.1 to 0.5% and sulfur close to 0.1%.

According to McKendry (2002), biomass samples with a carbon content around 20.0%, and an oxygen content close to 70.0%, present low energy density, since the greater proportion of oxygen and hydrogen, in comparison to the carbon, reduces the energy density of a fuel, due to the lower energy contained in C-O and C-H bonds, in relation to C-C bonds.

The H and N contents were found around 3.5 and 6.3%, respectively, *i.e.*, outside the range proposed by Telmo et al. (2010). These amounts, together with the carbon content previous reported are due to the presence of collagen, which is predominant in the fish scales (Santos, 2008). The sulfur level observed was less than 1.0%, with agrees with the reported by Kazanc et al. (2011) for organic feedstock. Since SO_x emissions are directly related to the sulfur amount present in biofuels, the low sulfur content can contribute to the reduction of greenhouse gas emissions (Cruz, 2015).

Table 2: Ultimate analysis for the different biomasses.

Biomasses	C (%)	H (%)	N (%)	S (%)	O (%)*	O (%)**
Fish scales	20.32±0.00	3.52±0.00	6.31±0.00	0.79±0.00	69.06±0.00	11.82±0.00
Sugarcane bagasse	45.05±0.00	5.57±0.00	0.25±0.00	n.d.	49.13±0.00	38.43±0.00
Scrubland pruning	33.11±0.00	3.90±0.00	1.19±0.00	0.25±0.00	61.56±0.00	21.55±0.00
Pea husk	24.51±0.00	0.27±0.00	0.42±0.00	1.00±0.00	73.80±0.00	58.50±0.00

O* = 100 - (%C + %H + %N + %S)

O** = 100 – (%C + %H + %N + %S + %moisture + %ash)

n.d. = not detected or below of the equipment detection limit

Source: adapted from Cruz (2015) and Garcia et al. (2012)

3.3 Calorimetry

Table 3 shows the average values and respective standard deviation for HHV and LHV (calculated based on the experimental HHV) for the fish scales and other biomass samples available in literature.

Table 3: Average values of HHV and LHV for the different biomasses.

Biomasses	HHV (MJ kg^{-1})	LHV (MJ kg^{-1})
Fish scales	9.08 ±0.02	8.17±0.00
Sugarcane bagasse	17.50±0.10	16.30±0.00
Scrubland pruning	12.88±0.60	11.92±0.00
Pea husk	14.46±0.00	14.14±0.00

Source: adapted from Cruz (2015) and Garcia et al. (2012)

The fish scales showed lower values for the experimental HHV (9.08 MJ kg^{-1}) and LHV (8.17 MJ kg^{-1}), when compared to others biomasses available in literature (Cruz, 2015; Garcia et al., 2012). These values can possibly be attributed to the low compositional carbon and hydrogen contents, as well as the low volatile materials content, as observed to the proximate and ultimate analyses. The high elemental oxygen content is also another important parameter that needs to be taken into account, since this element in large quantities reduces the Higher Heating Value (HHV) of a fuel due to the high bond enthalpy values (Atkins and Jones, 2012), requiring greater activation energies for breaking the bonds formed by the oxygen atoms (Braz and Crnkovic, 2014).

Among lignocellulosic materials presented in this study, ones that came closest to the HHV values obtained for the fish scales were scrubland pruning and pea husk, *e.g.*, 12.88 and 14.46 MJ kg^{-1}, respectively (Musellin et al., 2018; García et al., 2012). These samples presented similar carbon and oxygen compositions; however, were different in other aspects, for example, hydrogen composition and volatile materials.

3.4 Thermal Analysis (TG/DTG and DTA)

Figure 3 (a-b) shows the TG/DTG and DTA curves for the fish scale samples under combustion atmosphere, indicating the main stages of mass loss events. Initially, it was observed a moisture loss 13.66% at the temperature range from 30 to 205 °C. These results are in accordance with the proximate analysis (11.34%) and were similar

(13.00%) to the obtained by Ikoma et al. (2003), which studied *Pagrus major* fish scales under similar conditions.

Fig. 3. (a) TG/DTG and (b) DTA curves for the fish scales samples under combustion or oxidizing atmosphere (synthetic air: N_2/O_2: 80/20%).

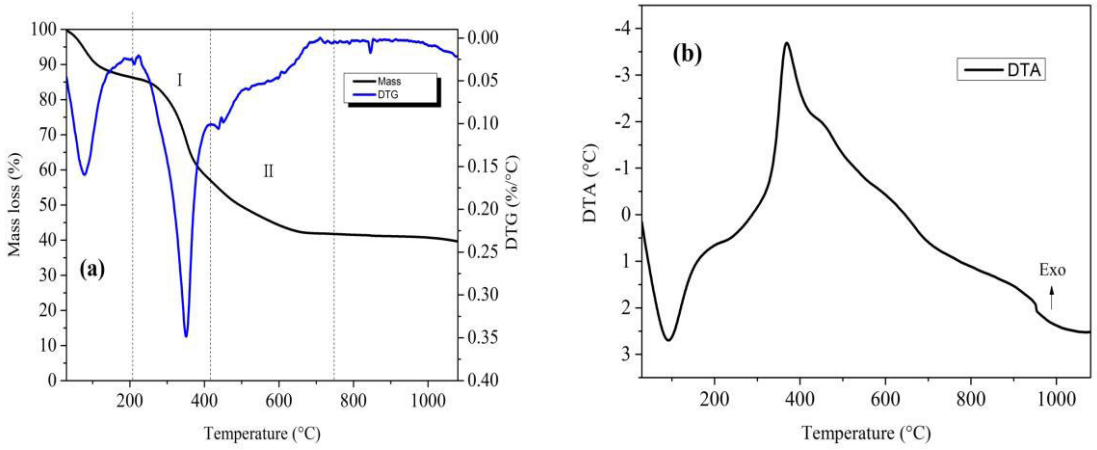

The second temperature range (between 205 and 416 °C) refers to the loss of organic matter, approximately 29.16%. This value is close to that previously determined by ultimate analysis (≈ 30.15%). In stage I of the thermal decomposition, the peak observed in DTG curve represents the maximum combustion rate at approximately 350 °C (Cruz et al., 2018), responsible for the largest mass loss event for the fish scale samples.

Stage II presented a mass loss of 15.38% and occurred between 416 and 750 °C. This thermal degradation stage, when analyzed together with the proximate analysis (Figure 2), showed the decomposition of the organic matter present in volatile and fixed carbon components. The last temperature range, from 750 °C to 1000 °C presented a remaining percentage of 41.8% mass, being attributed entirely to the non-degraded inorganic matter at this temperature range, *i.e.,* refers to the ashes content (Table 1)

In study performed by Ikoma et al. (2003), the authors considered only a single thermal degradation stage, presenting components of moisture, organic and inorganic matter. Also stated that some biopolymers, *e.g.*, the long-chain and branched polysaccharides, can be present in the organic phase of the fish scales in small amounts.

Figure 3b shows the DTA curve for the fish scale samples, which is characterized by the occurrence of endothermic and exothermic events. The endothermic process (heat gain), related to the evaporation of absorbed moisture, is characterized by the peak

at 92 °C. However, the exothermic event (heat release) was observed from 330 °C to 670 °C, with a maximum peak at 370 °C and represents the thermal decomposition of the collagen fibers and other biopolymers present in the samples. These processes have also been described by Ikoma et al. (2003) and occurred at the temperature ranges similar to those observed in this work (Table 4).

Figure 4 (a-b) shows the TG/DTG and DTA curves obtained under inert atmosphere (100% N_2). The moisture loss (12.10% w/w) occurred in the temperature range from 35 to 220 °C. Stage I presented a mass loss percentage of 29.47% in the range between 220 and 540 °C, referring to the thermal degradation of organic matter. The percentage of mass remaining around 58.43% was attributed to inorganic matter, for example, hydroxyapatite (Santos, 2008).

Fig. 4. (a) TG/DTG and (b) DTA curves for the fish scale samples under inert or pyrolysis atmosphere (100% N_2).

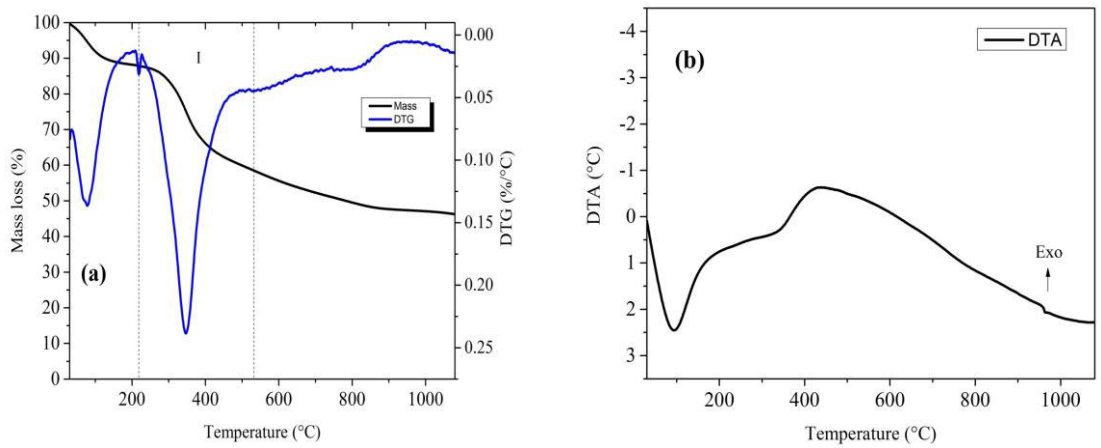

Figure 4b shows the DTA curve obtained for the (inert) pyrolysis atmosphere. The endothermic process was observed up to 230 °C, with a peak temperature at 94 °C, while the exothermic process presented a peak temperature at 435 °C and finished near 640 °C, this step was directly assigned to collagen fibers thermal decomposition (Santos, 2008).

Table 4 presents a summary from the temperature ranges and thermal degradation steps observed by means of the TG/DTG curves for the fish scales under inert and oxidizing atmospheres obtained in this work and compared to the results provided by Ikoma et al. (2003) and Santos (2008).

Table 4: Temperature ranges and thermal degradation steps extracted by means of TG/DTG curves under both atmospheres.

Biomasses	Atmospheres	Thermal degradation stages	Temperature ranges (°C)	Mass losses (%)
Fish scales (this study - Silva et al., 2019)	Synthetic air	Moisture loss	30 – 205	13.66±0.00
		Organic matter	205 – 416	29.16±0.00
		Organic and inorganic matter	416 – 750	15.38±0.00
		Inorganic matter	750	41.80±0.00
	100% N_2	Moisture loss	35 – 220	12.10±0.00
		Organic matter	220 – 540	29.47±0.00
		Inorganic matter	540	58.43±0.00
Fish scales of *Pagrus major* (Ikoma et al., 2003)	Synthetic air	Moisture loss	-	13.00±0.00
		Organic matter	-	41.00±0.00
		Inorganic matter	-	46.00±0.00
Fish scales of *Leporinus obtusidens* (Santos, 2008)	100% N_2	Moisture loss	30 – 230	13.00±0.00
		Organic matter	230 – 630	32.00±0.00
		Inorganic matter	630	55.00±0.00

Source: adapted from Ikoma et al. (2003) and Santos (2008)

It was observed that, despite difference between two atmospheres used, mass lost during moisture loss step was almost same (around 13%), but some difference were perceived in organic and inorganic matter contents, ranging from 29 to 44% and from 41 to 58%, respectively, for both atmospheres. All mass loss rates observed in this work were similar to the literature used as reference (Ikoma et al., 2003; Santos, 2008), as well as the different temperature ranges.

3.5 Energy Dispersive Spectroscopy (EDS)

Table 5 shows the EDS elemental composition for the fish scale samples, while Figure 5 the majority components. Some alkaline and alkaline earth metals such as Na,

Mg and Ca were identified. In real thermal processes, these elements can form oxides, hydroxides and carbonates, which are harmful to the combustion process and/or thermal plants operation, causing heat transfer problems (Fernández et al., 2012). However, these trace elements presented low levels in relation to the other fish scales components, as shown in Table 5.

Table 5: Percentage of the main inorganic and metallic compounds for the fish scales.

Sample	C (%)	O (%)	Na (%)	Mg (%)	Al (%)	P (%)	S (%)	Ca (%)
Fish scales	47.01±3.93	42.67±2.76	0.23±0.05	0.20±0.06	0.12±0.02	4.24±0.89	0.16±0.01	5.36±1.48

It was observed from Figure 5 that the majority components are carbon and oxygen (47.0 and 42.0%, respectively), followed by calcium and phosphorus (5.0 and 4.0%, respectively) in smaller amounts. Other trace elements such as Na (0.23%), Mg (0.20%), Al (0.12%) and S (0.16%) presented compositions below 1%. Other elements such as Fe, Si and K were not identified or quantified by this analysis.

Fig. 5. Main components present in the fish scales obtained by EDS analysis.

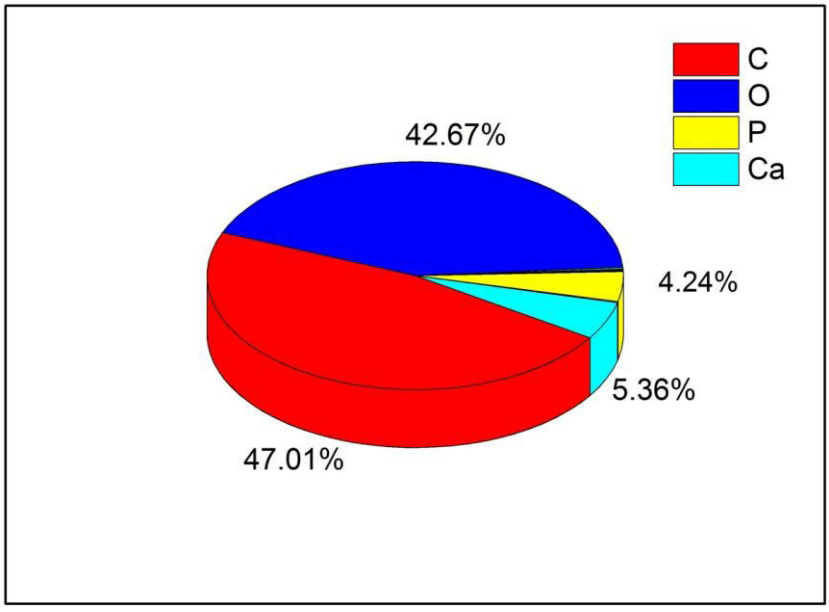

Ikoma et al. (2003) characterized the *Pagrus major* scales and suggested an inorganic composition of P_2O_5 (phosphorus pentoxide), Na_2O (sodium oxide), MgO (magnesium oxide), CaO (calcium oxide) and $Ca_{10}(PO_4)_6(OH)_2$. This latter component is known as hydroxyapatite, a phosphate constituted by three main elements: calcium, phosphorus and oxygen. According to Costa et al. (2009), the skeletons of some marine

species are main sources of this mineral, because contain calcium carbonate, but most of these species also present calcium phosphate. Mavropoulos (1999) stated that skeletons not reabsorbed in the life cycle of animals or marine carnivorous are deposited in the bottom of seas, oceans, lakes and lagoons, forming geological minerals deposits.

3.6 Determination of metal composition (ICP-OES)

Table 6 shows concentrations of the main metal and inorganic elements quantified for the fish scales samples by ICP-OES analysis, while Figure 6 shows major components present in these same structures .

Table 6: Chemical composition of collagenous biomass evaluated by ICP-OES (mg kg^{-1}).

Sample	Ba	B	Si	P	Mg	Ca	Na	K	Li	Zn	Cr	Fe	Pb	Mn	Al	Cu
Fish scales	7	9	27	75062	2499	164534	1677	180	1	65	3	48	6	11	27	11

The main components obtained by the ICP-OES analysis were Ca (67.39%), P (30.74%), Mg (1.02%) and Na (0.69%). Other metallic elements presented concentrations less than 1% of the total composition. These elements compared to other biomasses, such as sugarcane bagasse and rice husks (Cruz, 2015) presented high compositional values, mainly calcium (164,534 mg kg^{-1}) and phosphorus (75,062 mg kg^{-1}). It is interesting to note that by burning fossil fuels together with materials rich in calcium oxides (CaO), which also act as catalyst for the complex combustion reactions, these compounds act directly for decreasing in the carbon dioxide (CO_2)emissions generated by combustion of these non-renewable fuels (Roy et al., 2014; Werther et al., 2000).

Fig. 6. Main components present in the fish scales and measured by ICP-OES analysis.

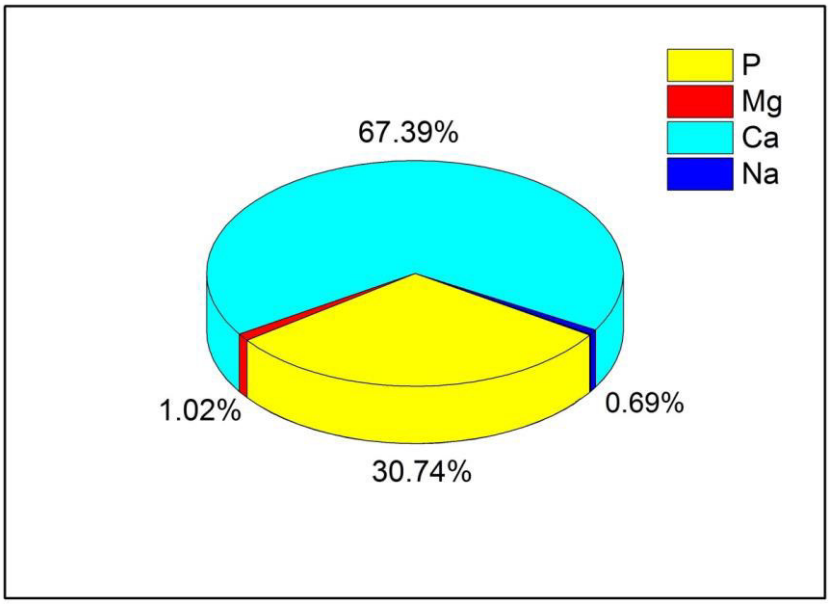

According Yuan et al (2019), during combustion or pyrolysis of biomass, the Ca-rich wastes could slightly influence the decomposition rate in the devolatilization stage at relatively lower temperatures (< 400 °C).

The Si, K, Na, P, Ca, Mg and Fe elements are directly involved in complex combustion reactions and also lead to the fouling formation, ash, slag and agglomerates in thermal plants (Jenkins et al., 1998). The phosphorus element is stable at low temperatures, causing the corrosion of furnaces and boilers, as well as contributing to the formation of atmospheric pollutants in thermochemical systems (Amonette and Joseph, 2009).

3.7 Fourier Transform Infrared Spectroscopy (FTIR)

The FTIR spectra obtained for the samples of fish scales are shown in Figure 7. These spectra showed similar absorption profiles for both particle sizes, but with some differences in intensities.

The absorption bands observed at 3597 and 2946 cm^{-1} are assigned, respectively, to the OH bonds and molecular vibrations from the CH_2 group (Rigo et al., 2007; Santos, 2008). The absorption peaks in the region between 3300 and 3480 cm^{-1} correspond to the NH stretching frequency. This vibration generally occurs in the range from 3400 to 3440 cm^{-1}, however, when NH group of a peptide is involved in a

hydrogen bond, this position is shifted to a lower frequency, *i.e.*, around 3300 cm^{-1} (Bhagwat and Dandge, 2016, Paul et al., 2017, Veeruraj et al., 2013).

The peaks in the range from 2300 to 2400 cm^{-1} were attributed to the C=O bonds of the CO_2 group (Kok et al., 2017; Musellim et al., 2018). The three bands observed at 1668, 1550 and 1245 cm^{-1} correspond to amides type I, II and III, respectively, and belong to type I collagen (Ikoma et al., 2003; Pati et al., 2010; Santos, 2008). Amide type I was associated to the stretching vibrations of the carbonyl groups (Payne and Veis, 1988). The amides II and III are resulting of the interactions between the angular deformations of NH and axial of CN, confirming the collagen helical triple structure (Plepis et al., 1996; Santos, 2008).

Peaks at 1439 and 864 cm^{-1} correspond to the CO bond of the carbonate groups incorporated into the apatite structure. The absorption bands at 1060 and 576 cm^{-1} are associated to the vibrational mode of the phosphate ions in hydroxyapatite framework (Ikoma et al., 2003; Rigo et al., 2007; Santos, 2008).

Fig. 7. Infrared spectrometers by Fourier Transform for the fish scales.

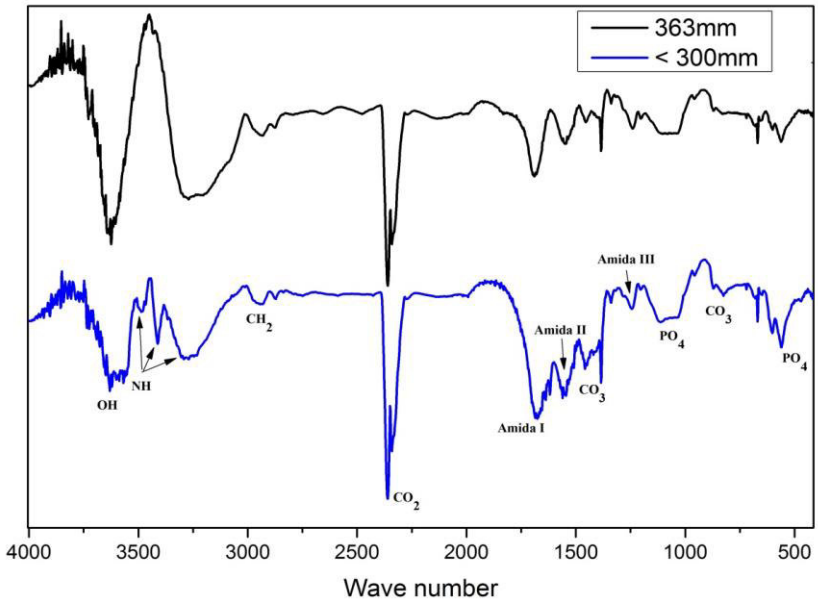

The results indicated that fish scales can form nanocomposites, consisting of collagen type I, carbonate ions and calcium deficient apatite (Ikoma et al., 2003).

3.8 X-Ray Diffraction (XRD)

The X-Ray diffractograms for the two particle sizes of the fish scales samples are shown in Figure 8. Six broad reflections were observed, corresponding to the angles at the 2θ scale equals to 26.03; 32.25 (higher intensities), 39.72; 46.76; 49.63 and 53.29. Despite the differences in particle sizes, it was also observed that both curves showed same crystallographic behavior in its structures.

Fig. 8. X-Ray diffractograms for the fish scales samples.

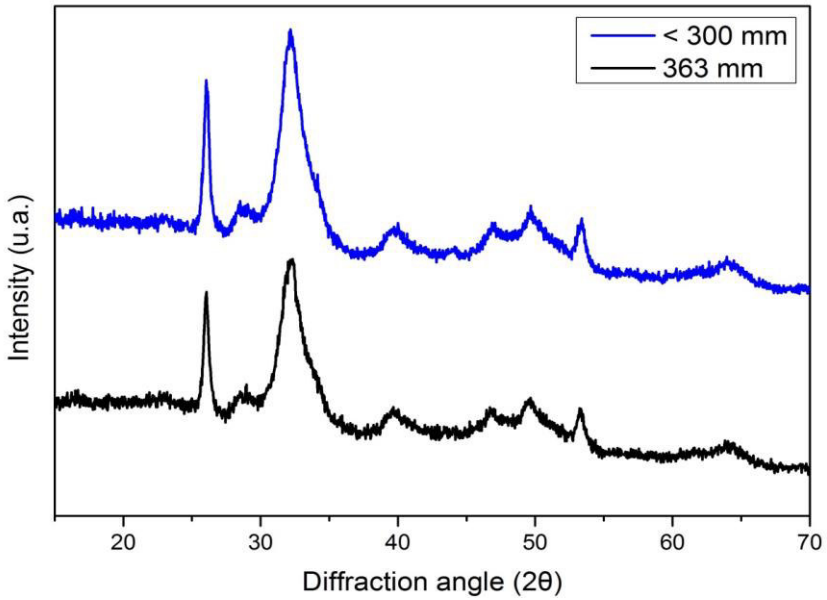

The values obtained for the interplanar spacings for the fish scales were 0.342; 0.278; 0.227; 0.194; 0.184 and 0.172 nm, respectively and corroborated to the values determined by Ikoma et al. (2003) and Santos (2008). According to Ikoma et al. (2003) and Santos (2008), these interplanar spacings correspond to the hydroxyapatite structure. The high and little intense diffraction peaks have suggested that crystals formed in this material may be small and/or structurally disordered, with possibility of low crystallinity (Ikoma et al., 2003; Santos, 2008).

The crystallinity index (CI) calculated for the fish scales was ≈ 10.9%, well below the values found for other known biomasses, for example, sugarcane bagasse (64.8%), coffee husk (57.7%), rice husk (53.0%) and nuts husk (63.8%) (Cruz et al., 2018; Sasmal et al., 2012). In thermochemical processes, amorphous product presents a higher reactivity when compared to the crystalline product (Xu et al., 2013). This absence of crystalline agglomerates or crystallinity makes the material more susceptible to the

complex reactions of thermal degradation during a combustion process, for example (Martinez et al., 2019).

3.9 Scanning Electron Microscopy (SEM images)

The images obtained by MEV are shown in Figure 9 (a-c) and the morphological characteristics of the fish scales were analyzed by three different magnifications (200, 500 and 1000 times).

Fig. 9. SEM micrographs for the fish scales with amplitudes: (a) 200, (b) 500 and (c) 1000 times.

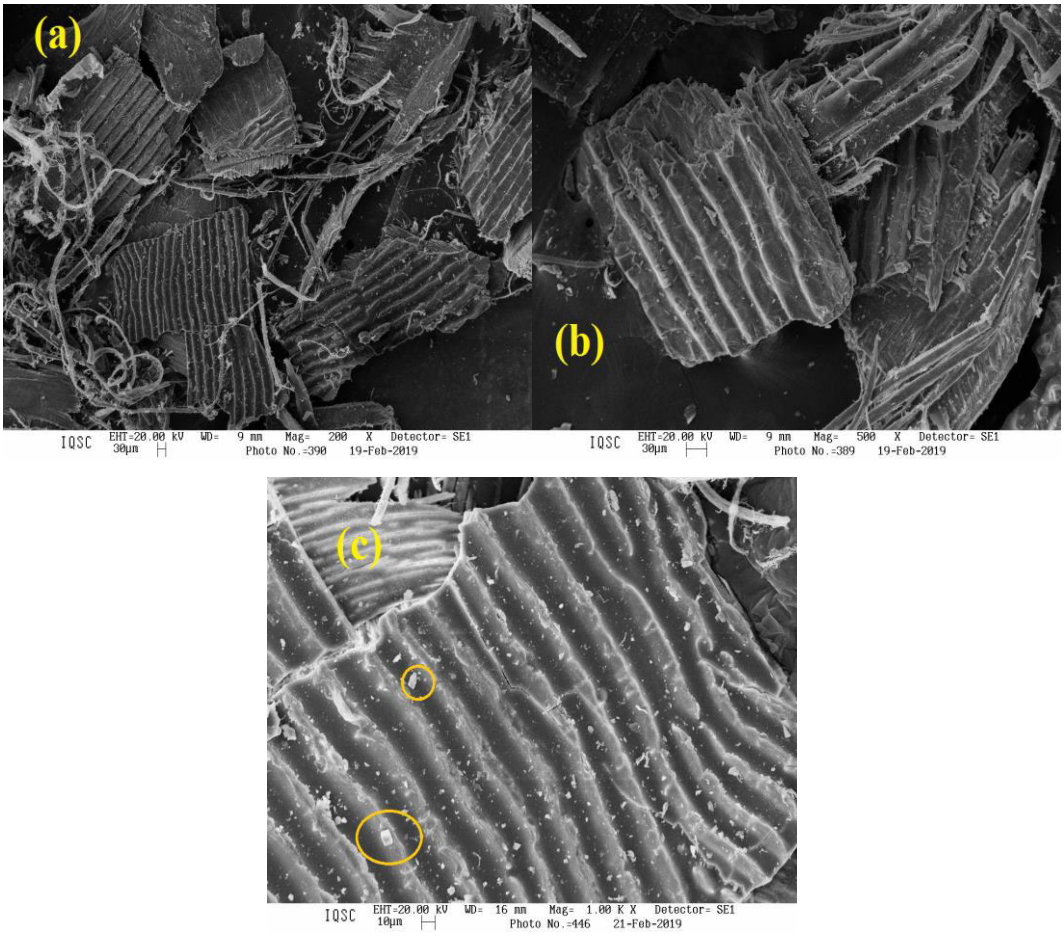

In Figure 9 (a-b) it was possible to observe a disorder in the fish scales structure. This disorder can have occurred due to the sample milling process, which can cause breakage in tubular structures, pores destruction and lamellae (Cruz, 2015). In Figure 9a it was possible to observe the presence of some fibers, lamellae and possibly residual collagen (Ikoma et al., 2003).

The amorphous behavior suggested by X-Ray analysis was verified and confirmed more clearly by Figure 9b. Figure 9c presented more details about the lamellae found, where it was possible to observe a well-ordered undulating morphology, following the parallel grooves shape similar to those observed to the rice husk samples (Cruz, 2015; Zhang et al., 2011).

It was also possible to show by means of Figure 9c some crystals presence and dispersed materials on the samples surfaces. These crystals present an apparently hexagonal organization (see yellow circles), which can be a strong characteristic of hydroxyapatite formation (Deer et al., 2000), confirming the presence of this important mineral in the fish scales.

4) Conclusions

This study evaluated the thermal behavior, physical-chemical properties, morphological and structural of fish scales in order to propose the application of this biomass as an alternative energy source in thermoconversion processes (combustion and pyrolysis) for the clean energy generation. The biomass presented good characteristics, such as calorific value, low sulfur content and considerable amount of calcium, which suggests a low emission of pollutants. However, the samples presented some metals in their composition (phosphorus, sodium and magnesium, in greater quantity) and high ash content in comparison to other materials, requiring a detailed study on these aspects. Finally, with this advanced characterization, it was possible for evaluating the fish scales and compares them with other biomasses already studied from an energetic view point, providing information for subsequent using of this feedstock in thermochemical reactors.

Acknowledgements

The authors gratefully acknowledge Foundation for Research Support, Scientific and Technological Development of Maranhão - FAPEMA (04989/18) and National Council for Scientific and Technological Development - CNPq (426162/2018-8) for the financial support. Environmental Sciences Laboratory (LACAM) of the Ceuma University, Mercedes-Benz Brazil for the ICP-OES analysis and Federal University of Maranhão for technical and professional support.

References

Almeida, Z.S., 2008. Os recursos pesqueiros marinhos e estuarinos do Maranhão: biologia, tecnologia, socioeconômica, estado da arte e manejo. Universidade Federal do Pará - Museu Paraense Emílio Goledi, 286 p.

Amonette, J.E., Joseph, S., 2009. Biochar for environmental management: science and technology. Earthscan, 33-52.

Associação Brasileira da Piscicultura (ABP). Anuário Peixe BR da Piscicultura. São Paulo, 2018.

ASTM E711, 1987. Standard Test Method for Gross Calorific Value of refuse – Derived Fuel by the Bomb Calorimeter.

Atkins, P., Jones, L., 2012. Princípios de Química. Bookman.

Babu, B.V., 2008. Biomass pyrolysis: a state-of-the-art review. Biofuels, Bioproducts and Biorefining 2 (5), 393-414.

Bhagwat, P.K., Dandge, P.B., 2016. Isolations, characterization and valorizable applications of fish scale collagen in food and agriculture industries. Biocatalysis and Agricultural Biotechnology 7, 234-240,

Braz, C.E.M., Crnkovic, P.M., 2014. Physical-chemical characterization of biomass samples for application in pyrolysis process. Chemical Engineering Transactions 37, 523-528.

Callister, W.D., 2002. Ciência e Engenharia de Materiais: Uma Introdução. LTC, 37-39.

Chen, W.H., Kuo, P.C., 2011. Torrefaction and co-torrefaction characterization of hemicellulose, cellulose and lignin as well as torrefaction of some basic constituents in biomass. Energy 36 (2), 803-811.

Costa, A.C.F.M., Lima, M.G., Lima, L.H.M.A., Cordeiro, V.V., Viana, K.M.S., Souza, C.V., Lira, H.L., 2009. Hidroxiapatita: obtenção, caracterização e aplicações. Revista Eletrônica Mater, 29-38.

Cortez, L.A.B., Lora, E.E.S., Gomez, E.O., 2008. Biomassa para Energia. Unicamp.

Cruz, G., 2015. Características físico-químicas de biomassas lignocelulósicas e a correlação entre suas emissões e os resíduos gerados sob diferentes condições

atmosféricas em um forno tubular de queda livre (DTF). Escola de Engenharia de São Carlos, Universidade de São Paulo, 273 p.

Cruz, G., Braz, C.E.M., Avila, I., Crnkovic, P.M., 2018. Physico-chemical properties of Brazilian biomass: Potential applications as renewable energy source. African Journal of Biotechnology, 1-19.

Cruz, G., Crnkovic, P.M., 2019. Assessment of the physical-chemical properties of residues and emissions generated by biomass combustion under N_2/O_2 and CO_2/O_2 atmospheres in a Drop Tube Furnace (DTF). Journal of Thermal Analysis and Calorimetry, 1-15.

Daboor, S.M. et al., 2012. Isolation and activation of collagenase from fish processing waste. Bioscience and Biotechnology 3, 191-203.

DB-CITY., 2019. Geografia São Luís. Available: < https://pt.db-city.com/Brasil--Maranh%C3%A3o--S%C3%A3o-Lu%C3%ADs>. (Access: 19.mar.19).

Deer, W.A., Howie, R.A., Zussman, J., 2000.Minerais Constituintes das rochas: Uma introdução. Fundação Calouste Gulbenkian, 683-688.

Brasil – Bazilian Energy Balance, 2018, Year 2017. Enterprise of Energy Research – Rio de Janeiro: EPE 294 p. Available: <https://ben.epe.gov.br/downloads/Relatorio_Final_BEN_2018.pdf>. Access: 18.mar.19.

Fernández, R.G. et al., 2012. Study of main combustion characteristics for biomass fuels used in boilers. Fuel Processing Technology 103 (1), 16-26.

García, R. et al., 2012. Characterization of Spanish biomass wastes for energy use. Bioresource Technology 103 (1), 249-258.

Foletto, E.L. et al., 2005. Aplicabilidade das cinzas da casca de arroz. Química Nova 28 (6), 1055-1060.

Ghaly, A.E., Ramakrishnan, V.V., Brooks, M.S., Budge, S.M., Dave, D., 2013. Fish processing wastes as a potential source of proteins, aminoacids and oils: a critical review. Journal of Microbial and Biochemical Technology 5, 107–129.

Ghetti, O., Ricca, L., Angelini, L., 1996. Thermal analysis of biomass and corresponding pyrolysis products. Fuel 75 (5), 565–573.

Huang, C.Y., Kuo, J.M., Wu, S.J., Tsai, H.T., 2016. Isolation and characterization of fish scale collagen from tilapia (*Oreochromis sp*.) by a novel extrusion-hydro extraction process. Food Chemistry 190, 997–1006.

Ikoma, T., Kobayashi, H., Tanaka, J., Walsh, D., Mann, S., 2003. Microstructure, mechanical, and biomimetic properties of fish scales from *Pagrus major*. International Journal of Biological Macromolecules 32, 199-204.

Jenkins, B.M. et al., 1998. Combustion properties of biomass. Fuel Processing Technology 54 (1-3), 17-46.

Jun, S. et al., 2004. Purification an characterization of an antioxidative peptide from enzymatic hydrolysate of yellowfin sole (*limanda aspera)* frame protein. European Food Research and Technology 219 (1), 20-26.

Kazanc, F. et al., 2011. Emissions of NO_x and SO_2 from coals of various ranks, bagasse, and coal bagasse burning in O_2/N_2 and O_2/CO_2 environments. Energy and Fuels 25 (7), 2850-2861.

Khan, A.A., De Jong, W., Jansens, P.J., Splithoff, H., 2009. Biomass combustion in fluidized bed boilers: potential problems and remedies. Fuel Processing Technology 90, 21–50.

Kok, M.V., Varfolomeev, M.A., Nurgaliev, D.K., 2017. Crude oil characterization using TGA-DTA, TGA-FTIR and TGA-MS techniques. Journal of Petroleum Science and Engineering 154, 537-542.

Leite, S.B.P. et al., 2016. Resíduos da comercialização de pescado marinho: volume de descarte e aspectos microbiológicos. Revista Brasileira de Tecnologia Agroindustrial 10 (1), 2112-2125.

Lela, B., Barisic, M., Nizetic, S., 2016. Cardboard/sawdust briquettes as biomass fuel: Physical-mechanical and thermal characteristics. Waste Management, 47 (B), 236-245.

Leroy, V., Cancellieri, D., Leoni, E., 2006. Chemical and thermal analysis of lingo-cellulosic fuels. Forest Ecology and Management 234S, S125.

Martinez, C.L.M., Rocha, E.P.A., Carneiro, A.C.O., Gomes, F.J.B., Batalha, L.A.R., Vakkilainen, E., Cardoso, M., 2019. Characterization of residual biomasses from the coffee production chain and assessment the potential for energy purposes. Biomass and Bioenergy 120, 68-76.

Martins, M.E.O., Claudino, R.L., Morais, J.P.S., Cassales, A.R., Alexandre, I.C., Souza, B.W.S., Alcântara, L.O., Sousa, J.R., Souza Filho, M.S.M., 2015. Obtenção de gelatina a partir de escama de tilápia (*Oreochromis niloticus*): Características químicas e físico-químicas. Boletim de Pesquisa Embrapa 108.

Mavroupoulos, E., 1999. A hidroxiapatita como removedora de chumbo. Fundação Oswaldo Cruz, Escola Nacional de Saúde Pública e Toxicológica, 126 p.

Mckendry, P., 2002. Energy production from biomass (part 1): overview of biomass. Bioresource Technology 83 (1), 37-46.

Melo, C.E., Ropke, C.P., 2004. Alimentação e distribuição de piaus (*Pisces anastomidae*) na Planície do Bananal, Mato Grosso, Brasil. Revista Brasileira de Zoologia 21, 51-56.

Musellim, E., Tahir, M.H., Ahmad, M.S., Ceylan, S., 2018. Thermokinetic and TG/DSC-FTIR study of pea waste biomass pyrolysis. Applied Thermal Engineering 137, 54-61.

NBR 8633, 1984. Carvão vegetal – Determinação do Poder Calorífico.

Paul, S., Pal, A., Choudhury, A.R., Bodhak, S., Balla, V.K., Sinha, A., Das, M., 2017. Effect of trace elements on the sintering effect of fish scale derived hydroxyapatite and its bioactivity. Ceramics International 43, 15678-15684.

Pati, F., Adhikari, B., Dhara, S., 2010. Isolation and characterization of fish scale collagen of higher thermal stability. Bioresource Technology 101, 3737–3742.

Payne, K.J., Veis, A., 1988. Fourier transform IR spectroscopy of collagen and gelatin solutions: deconvolution of the amide I band for conformational studies. Biopolymers 27 (11), 1749–1760.

Permchart, W., Kouprianov, V.I., 2004. Emission performance and combustion efficiency of a conical fluidized-bed combustor firing various biomass fuels. Bioresource Technology 92 (1), 83-91.

Pickler, E., Filho, J.E.R.V., 2017. Evolução da piscicultura no Brasil: Diagnóstico e desenvolvimento da cadeia produtiva de tilápia. Textos para discussão - IPEA, agosto de 2017. Available: <http://www.ipea.gov.br/portal/images/stories/PDFs/TDs/td_2328.pdf>. Access: 10.mar.19.

Plepis, A.M.G., Goissis, G., Das-Gupta, D.K., 1996. Dielectric and pyroelectric characterization of anionic and native collagen. Polymer Engineering and Science 36, 2932–2938.

Poletto, M., Zattera, A.J., Santana, R.M.C., 2012. Thermal decomposition of wood: kinetics and degradation mechanisms. Bioresource Technology 126, 7-12.

Raveendran, K., Ganesh, A.,Khilart, K.C., 1995. Influence of mineral matter on biomass pyrolysis characteristics. Fuel 74 (12), 1812-1822.

Rigo, E.C.S., Gehrke, S.A., Carbonari, M., 2007. Síntese e caracterização de hidroxiapatita obtida pelo método da precipitação. Revista Dental Press Periodontia Implantol 1 (3), 39-50.

Roy, M.M., Corscadden, K.W., 2012. An experimental study of combustion and emissions of biomass briquettes in a domestic wood stove. Applied Energy 99 (1), 206-212.

Roy, Y. et al., 2014. Biomass combustion for greenhouse carbon dioxide enrichment. Biomass and Bioenergy 66 (1), 186-196.

Saidur, R. et al., 2011. A review on biomass as a fuel for boilers. Renewable and Sustainable Energy Reviews 15 (5), 2262-2289.

Saddawi, A. et al., 2010. Kinetics of the thermal decomposition of biomass. Energy and Fuels 24 (2), 1274-1282.

Sanchez-Silva, L. et al., 2012. Thermogravimetric-mass spectrometric analysis of lignocellulosic and marine biomass pyrolysis. Bioresource Technology 109 (1), 163-172.

Santos, E.B., 2008. Caracterização de escamas do peixe Piau (*Leporinus elongatus*) e sua aplicação na remoção de íons Cu(II) em meio aquoso. Universidade Federal de Sergipe, 90 p.

Sasmal, S., Goud, V.V., Mohanty, K., 2012. Characterization of biomasses available in the region of North-East India for production of biofuels. Biomass and Bioenergy 45, 212-220.

Sockalingam, K., Abdullah, H.Z., 2015. Extraction and characterization of gelatin biopolymer from black tilapia (*Oreochromismos sambicus*) scales. AIP Conference Procedings.

Spliethoff, H., 2010. Power generation from solids fuels. 38th Springer-Verlag: Berlin.

Svoboda, K. et al. 2009. Pretreatment and feeding of biomass for pressurized entrained flow gasification. Fuel Processing Technology 90 (5), 629-635.

Telmo, C., Lousada, J., Moreira, N., 2010. Proximate analysis, backwards step wise regression between gross calorific value, ultimate and chemical analysis of wood. Bioresource Technology101 (11), 3808-3815.

Torquato, L. et al., 2017. New approach for proximate analysis by thermogravimetry using CO_2 atmosphere: validation and application to different biomasses. Journal of Thermal Analysis and Calorimetry 128, 1-14.

Veeruraj, A., Arumugam, M., Balasubramanian, T., 2013. Isolation and characterization of thermostable collagen from the marine eel-fish (*Evenchelys macrura*). Process Biochemistry 48 (10), 1592-1602.

Wang, J. et al., 2006. A comparative study of thermolysis characteristics and kinetics of seaweeds and fir wood. Process Biochemistry 41 (8), 1883-1886.

Werther, J. et al., 2000. Combustion of agricultural residues. Progress in Energy and Combustion Science 26 (1), 1-27.

Williams, A. et al., 2012. Pollutants from the combustion of solid biomass fuels. Progress in Energy and Combustion Science 38 (2), 113-137.

Xu, F., Shi, Y., Wang, D., 2013. X-Ray scattering studies of lignocellulosic biomass: a review. Carbohydrate Polymers 94, 904-917.

Yang, H. et al., 2007. Characteristics of hemicelulose, cellulose and lignin pyrolysis. Fuel 86 (12-13), 1781-1788.

Yao, B.Y., Changkook, R., Adela, K., Yates, N.E., Sharifi, V.N., Swithenbank, J., 2005. Effect of fuel properties on biomass combustion. Part II. Modelling approach identification of the controlling factors. Fuel 84 (16), 2116-2130.

Yu, C.T., Chen, W.H., Men, L.C., Hwang, W.S., 2009. Microscopic structure features changes of rice straw treated by boiled acid solution. Industrial Crops and Products 29, 308-315.

Yuan, R., Yu, S., Shen, Y., 2019. Pyrolysis and combustion kinetics of lignocellulosic biomass pellets with calcium-rich wastes from agro-forestry residues. Waste Management 87, 86-96.

Zhang, F. et al., 2011. Preparation and characterization of collagen from freshwater fish scales. Food and Nutrition Sciences 2, 818-823.